

# Collisions in zero temperature Fermi gases

Subhadeep Gupta, Zoran Hadzibabic, James R. Anglin, and Wolfgang Ketterle

*Department of Physics, MIT-Harvard Center for Ultracold Atoms, and Research Laboratory of Electronics, MIT, Cambridge, MA 02139*

(June 26, 2018)

We examine the collisional behavior of two-component Fermi gases released at zero temperature from a harmonic trap. Using a phase-space formalism to calculate the collision rate during expansion, we find that Pauli blocking plays only a minor role for momentum changing collisions. As a result, for a large scattering cross-section, Pauli blocking will not prevent the gas from entering the collisionally hydrodynamic regime. In contrast to the bosonic case, hydrodynamic expansion at very low temperatures is therefore not evidence for fermionic superfluidity.

PACS numbers: 03.75.Ss, 03.75.Kk, 34.50.-s

The last few years have seen rapid progress in the field of ultracold atomic Fermi gases [1–6]. Most recently, regimes of strong interactions have been observed in these gases near Feshbach resonances [7–10]. Studies of these systems are of particular importance because of the possibility of creating BCS-like superfluids [11,12]. Such a realization would establish highly controllable model systems for studying novel regimes of fermionic superfluidity.

A unique feature of atomic systems is the ability to analyze the gas by turning off the trapping potential and observing the expansion. The expansion behavior can reveal the momentum distribution and the effects of mean-field interactions and collisions. Hydrodynamic behavior can be easily detected when the gas is released from an anisotropic atom trap. In that case, the spatial anisotropy of the cloud reverses during free expansion. This is caused by the larger pressure gradient along the tightly confining direction, which leads to a faster expansion, and subsequent reversal of the spatial anisotropy. This anisotropic expansion was used to identify the formation of the Bose-Einstein condensate [13,14].

A BEC obeys the hydrodynamic equations of a superfluid [15]. However collisional hydrodynamics arising from a high elastic collision rate also results in anisotropic expansion [16,17]. Thus, the normal component can also expand anisotropically [18]. For the bosonic case, two key points make the distinction between the two fractions obvious: (i) At the typical transition temperature, the BEC has much less energy than the normal cloud, so the two components are clearly separated in size. (ii) The scattering rate needed to achieve condensation is usually not large enough that the normal gas is in the hydrodynamic regime. For these two reasons, the appearance of a dense anisotropic cloud during expansion is considered to be the “smoking-gun” for the formation of a Bose-Einstein condensate.

A superfluid Fermi gas is predicted to obey the superfluid hydrodynamic equations of motion [19–22] and therefore should show strong anisotropic expansion when released from an anisotropic harmonic trap [22]. The recent observation of anisotropic expansion of an ultracold,

interacting, two-spin fermionic mixture [7–9] has created considerable excitement and raised the question under what conditions is this expansion a signature of fermionic superfluidity and not of collisional hydrodynamics. There are two major differences from the bosonic case: (i) Since the energy of ultracold fermions always remains on the order of the Fermi energy, the size in expansion for both normal and superfluid components will be similar. (ii) Current efforts towards inducing BCS pairing all take place in strongly interacting systems. This results in a large scattering rate modified only by the effects of Pauli blocking at low temperatures.

The interpretation of the observed anisotropic expansion in strongly interacting Fermi gases is therefore critically dependent on the role of Pauli blocking of collisions during the expansion. The tentative interpretation of anisotropic expansion as superfluid hydrodynamics [7] was based on the assessment that collisions are strongly suppressed at sufficiently low temperatures [7,23–28].

Here we show generally that the collision rate becomes independent of temperature and prevails even at zero temperature, if the Fermi surface is strongly deformed. This happens in an extreme way during ballistic expansion. In the small cross-section limit, we find that less than half of the total number of momentum changing collisions is suppressed. For a large scattering cross-section, the absence of suppression results in strong collisional behavior of normal Fermi gases during expansion for all initial temperatures. This result has the important consequence of rendering expansion measurements of Fermi gases near Feshbach resonances ambiguous for differentiating between superfluid and normal components.

We first consider the expansion of a single component Fermi gas. At ultralow temperatures, fermionic antisymmetry prevents s-wave scattering in a single component and renders the gas completely collisionless. The phase space occupation  $f(x_1, x_2, x_3, p_1, p_2, p_3) = f(\mathbf{x}, \mathbf{p})$  at zero temperature in a harmonic trap with frequencies  $(\omega_1, \omega_2, \omega_3)$  can be written as

$$f(\mathbf{x}, \mathbf{p}) = \Theta(E_F - \sum_i m\omega_i^2 x_i^2/2 - \sum_i p_i^2/2m)$$

where  $m$  is the particle mass,  $\Theta$  is the Heaviside step

function defined as  $\Theta(x) = 0(1)$  for  $x \leq 0(x > 0)$  and  $E_F = \hbar(6N\Pi_i\omega_i)^{1/3}$  is the Fermi energy for  $N$  particles. At time  $t = 0$ , the trapping potential is turned off suddenly, allowing the gas to expand freely. At  $t = 0$ , the momentum space Fermi surface at  $\mathbf{x} = (x_1, x_2, x_3)$  is

$$\Sigma_i p_i^2/2m = E_F - \Sigma_i m\omega_i^2 x_i^2/2, \quad (1)$$

a sphere of radius  $\sqrt{2m(E_F - \Sigma_i m\omega_i^2 x_i^2/2)}$ . In this non-interacting system, the evolution of the Fermi surface can be derived from the simple evolution law for ballistic expansion  $\mathbf{x}(0) = \mathbf{x}(t) - \mathbf{p}t/m$ . Substituting this in Eq. 1, we obtain:

$$\Sigma_i \frac{(1 + \omega_i^2 t^2)}{2m} \left( p_i - \frac{m x_i}{t} \frac{\omega_i^2 t^2}{1 + \omega_i^2 t^2} \right)^2 = E_F - \Sigma_i \frac{m\omega_i^2 x_i^2}{2(1 + \omega_i^2 t^2)}, \quad (2)$$

which is an ellipsoid with generally unequal axes  $\sqrt{2m(E_F - \Sigma_i \frac{m\omega_i^2 x_i^2}{2(1 + \omega_i^2 t^2)})} (\frac{1}{\sqrt{1 + \omega_1^2 t^2}}, \frac{1}{\sqrt{1 + \omega_2^2 t^2}}, \frac{1}{\sqrt{1 + \omega_3^2 t^2}})$ . The anisotropy of the Fermi surface during expansion can be understood generally by noting that for long times  $t$ , at any position  $\mathbf{x}$ , the spread in momentum  $\Delta p_i(t)$  can only arise from the initial spread in position  $\Delta x_i(0)$ . For anisotropic traps this gives rise to an anisotropic momentum distribution during ballistic expansion. For a mixture of two spin states, this deformation of the Fermi surface from a sphere into an anisotropic ellipsoid removes Pauli blocking of final states and allows collisions, as will be shown.

The momentum distribution at position  $\mathbf{x}$  given by Eq. 2, also allows us to simply calculate the spatial density distribution as the volume of the momentum-space ellipsoid,

$$n(\mathbf{x}, t) = \frac{4}{3}\pi \left( \frac{2mE_F}{h^2} \right)^{3/2} \frac{(1 - \frac{m}{2E_F} \Sigma_i \frac{\omega_i^2 x_i^2}{1 + \omega_i^2 t^2})^{3/2}}{\Pi_i (1 + \omega_i^2 t^2)^{1/2}}, \quad (3)$$

in agreement with other derivations [29]. For long expansion times  $t$ , the spatial distribution becomes isotropic, mirroring the isotropic momentum distribution in the trap.

Specializing to the experimentally relevant case of a cylindrically symmetric trap, ballistic expansion deforms the local Fermi surface into a momentum ellipsoid of cylindrical symmetry with aspect ratio  $\sqrt{\frac{1 + \omega_z^2 t^2}{1 + \omega_\perp^2 t^2}}$  (Fig. 1(a,b)). Here  $\omega_\perp$  ( $\omega_z$ ) is the radial (axial) trapping frequency. For long times  $t$ , this deformation reaches the asymptotic aspect ratio  $\omega_z/\omega_\perp = \lambda$ , the initial spatial aspect ratio in the trap.

Now consider an equal mixture of two spin states which interact via a finite s-wave scattering length. We assume that the trapping frequencies are identical for the two states (standard experimental conditions) and specialize to the usual case of two-body elastic collisions in the

local-density approximation. These collisions have an appealing geometrical picture in the local phase-space description (Fig. 1(c)). Each elastic collision involves one particle from each spin state. We label with  $\mathbf{p}$ 's and  $\mathbf{q}$ 's the momenta of the two different spin states. Consider the collision  $\mathbf{p}_1 + \mathbf{q}_1 \rightarrow \mathbf{p}_2 + \mathbf{q}_2$ . Conservation of momentum and kinetic energy mandates  $\mathbf{p}_2 + \mathbf{q}_2 = \mathbf{p}_1 + \mathbf{q}_1$  and  $|\mathbf{p}_2 - \mathbf{q}_2| = |\mathbf{p}_1 - \mathbf{q}_1|$ . These relations restrict  $\mathbf{p}_2$  and  $\mathbf{q}_2$  to lie on diametrically opposite ends of the sphere with  $\mathbf{p}_1 - \mathbf{q}_1$  as a diameter. The deformation of the Fermi surface during expansion opens up unoccupied final states  $\mathbf{p}_2, \mathbf{q}_2$  and therefore allows collisions to take place even in a zero temperature Fermi gas (Fig. 1(c)).

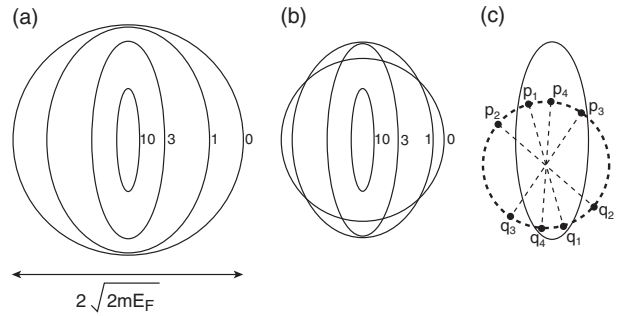


FIG. 1. (a) Deformation of the momentum space Fermi surface at  $\mathbf{x} = \mathbf{0}$ , from a sphere to an ellipsoid during expansion from an anisotropic harmonic trap. The case of cylindrical symmetry is shown, where the three-dimensional distribution is symmetric about the vertical axis. The parameters chosen are an aspect ratio  $\lambda = 0.2$  and expansion times  $\omega_\perp t = 0, 1, 3$  and 10. (b) The deformation at a position radially displaced by  $\sqrt{E_F/m\omega_\perp^2}$ . (c) Geometrical representation of collisions in momentum space. The two spin states have identical distributions. Three different types of collisions are shown for particles with initial momenta  $\mathbf{p}_1$  and  $\mathbf{q}_1$  - none, one or both of the final states are occupied.

The effect of collisions can be formally calculated from the Boltzmann transport equation for the evolution of the phase space distribution  $f(\mathbf{x}, \mathbf{p}, t)$ . In the absence of external potentials and neglecting mean field we have [30]:

$$\frac{\partial f}{\partial t} + \mathbf{v} \cdot \frac{\partial f}{\partial \mathbf{x}} = \Gamma_{\text{coll}}[f] \quad (4)$$

where  $\mathbf{v} = \mathbf{p}/m$  and  $\Gamma_{\text{coll}}[f]$  describes the effect of collisions. Collisions attempt to restore local equilibrium by countering the deformation of the momentum space Fermi surface during free expansion (Eq. 2).

$\Gamma_{\text{coll}}[f]$  can be written as the collision integral:

$$\Gamma(\mathbf{x}, \mathbf{p}_1, t) = -\frac{\sigma}{4\pi h^3} \int_{(\mathbf{x}, t)} d^3 q_1 d^2 \Omega \frac{|\mathbf{p}_1 - \mathbf{q}_1|}{m} \times \\ [f(\mathbf{p}_1)f(\mathbf{q}_1)(1 - f(\mathbf{p}_2))(1 - f(\mathbf{q}_2)) \\ - f(\mathbf{p}_2)f(\mathbf{q}_2)(1 - f(\mathbf{p}_1))(1 - f(\mathbf{q}_1))] \quad (5)$$

where  $\sigma$  is the momentum-independent scattering cross-section,  $f(\mathbf{p}_i) = f(\mathbf{x}, \mathbf{p}_i, t)$ ,  $f(\mathbf{q}_i) = f(\mathbf{x}, \mathbf{q}_i, t)$  and  $\Omega$  points along  $\mathbf{p}_2 - \mathbf{q}_2$ . The integral over  $\mathbf{q}_1$  is over the momentum ellipsoid at position  $\mathbf{x}$  and time  $t$  for one of the spin states. The first term in the integrand is the collision rate for the process  $\mathbf{p}_1 + \mathbf{q}_1 \rightarrow \mathbf{p}_2 + \mathbf{q}_2$ . The second term corresponds to the reverse process  $\mathbf{p}_2 + \mathbf{q}_2 \rightarrow \mathbf{p}_1 + \mathbf{q}_1$ , and ensures that only distribution changing collisions contribute.

Pauli blocking is expressed in the suppression factors for the final states  $(1 - f)$  in  $\Gamma$ . The collision integral neglecting Pauli blocking,  $\Gamma_{\text{Cl},p}$ , is furnished by setting the suppression factors all equal to 1 in Eq. 5. This is the rate for classical collisions which change the momentum distribution. The total classical collision rate  $\Gamma_{\text{Cl}}$  is the first term on the right hand side of Eq. 5 without any suppression factors. In addition to  $\Gamma_{\text{Cl},p}$ , this also contains the rate for collisions which do not change the momentum distribution: if both final states are occupied, then the reverse process has the same rate. These additional collisions do not affect observables of the system. Fig. 1(c) shows examples of these different types of collisions.  $\mathbf{p}_1 + \mathbf{q}_1 \rightarrow \mathbf{p}_2 + \mathbf{q}_2$  contributes to  $\Gamma_{\text{Cl}}$ ,  $\Gamma_{\text{Cl},p}$  and  $\Gamma$ .  $\mathbf{p}_1 + \mathbf{q}_1 \rightarrow \mathbf{p}_3 + \mathbf{q}_3$  contributes to  $\Gamma_{\text{Cl}}$  and  $\Gamma_{\text{Cl},p}$ .  $\mathbf{p}_1 + \mathbf{q}_1 \rightarrow \mathbf{p}_4 + \mathbf{q}_4$  contributes only to  $\Gamma_{\text{Cl}}$ . To determine the effect of Pauli blocking, we compare  $\Gamma$  and  $\Gamma_{\text{Cl},p}$  for a small cross-section  $\sigma$ . The collision rate at a particular time  $t$  can then be calculated perturbatively, by propagating the system ballistically for the time  $t$  and then evaluating Eq. 5 with and without the suppression factors.

Fig. 2(a) displays the numerically calculated collision rates  $\Gamma$ ,  $\Gamma_{\text{Cl},p}$  and  $\Gamma_{\text{Cl}}$ , evaluated at  $\mathbf{x} = \mathbf{p} = \mathbf{0}$ , as a representative case, for an initial aspect ratio  $\lambda = 0.03$ . Both  $\Gamma$  and  $\Gamma_{\text{Cl},p}$  increase initially as the deformation of the Fermi surface becomes more pronounced. For long times ( $\omega_{\perp} t \gg 1$ ), they are both suppressed because both the density ( $\int d^3 q_1$ ) and the relative velocity ( $\frac{|\mathbf{p}_1 - \mathbf{q}_1|}{m}$ ) drop. The two curves approach each other with time since Pauli blocking becomes less effective with stronger deformation. The fraction of momentum changing collisions which are not affected by Pauli blocking,  $F(\lambda) = \int dt \Gamma(\mathbf{0}, \mathbf{0}, t) / \int dt \Gamma_{\text{Cl},p}(\mathbf{0}, \mathbf{0}, t)$ , is shown in Fig. 2(b). The main result of our paper is the inefficiency of Pauli blocking during expansion from anisotropic traps. For  $\lambda < 0.05$ ,  $F > 0.5$ , and approaches  $\sim 0.55$  as  $\lambda$  approaches 0. Most experiments work in this regime of trap aspect ratio.

The above results form an upper bound on the Fermi suppression even if we consider all the possible collisions occurring in the system, for arbitrary  $\mathbf{x}$  and  $\mathbf{p}$ . First, we observe that for all  $\mathbf{x}$ , at any time  $t$ , the Fermi surface is identically deformed and different only in size according to the local density (Eqs. 2,3, Fig. 1(a,b)). We have checked numerically that to within 5%, the central mo-

mentum provides a lower bound on  $\Gamma$  within a momentum ellipsoid, at all  $\mathbf{x}$  and for all times  $t$ . Next, we note that for  $\mathbf{x} \neq \mathbf{0}$ , the density  $n(\mathbf{x}, t)$  puts more weight at longer times than  $n(\mathbf{0}, t)$  (Eq. 3). Since Fermi suppression becomes less effective with time, Pauli blocking is most effective at  $\mathbf{x} = \mathbf{0}$ . The calculation for  $\mathbf{x} = \mathbf{p} = \mathbf{0}$  thus provides an effective upper bound for the overall collisional suppression in the system. We conclude that more than half of all the possible collisions are not Pauli blocked for typical experimental values of  $\lambda$ .

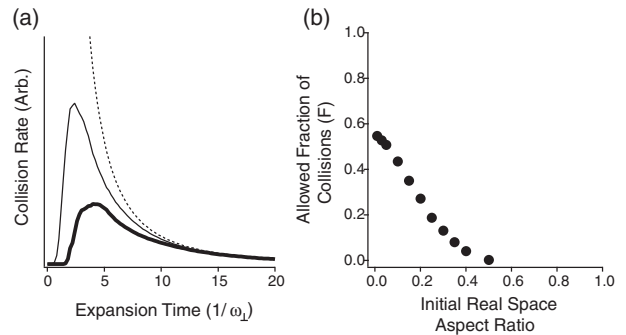


FIG. 2. (a) Collision rate as a function of expansion time in the perturbative approximation for the initial aspect ratio  $\lambda = 0.03$ . Dashed line - total classical collision rate  $\Gamma_{\text{cl}}$ , thin line - classical rate for momentum changing collisions  $\Gamma_{\text{cl},p}$ , thick line - collision rate for fermions  $\Gamma$ . The displayed rates were evaluated at  $\mathbf{x} = \mathbf{0}$  and  $\mathbf{p} = \mathbf{0}$  and give an effective upper bound on the Fermi suppression. (b) Allowed fraction of collisions  $F(\lambda)$  for a zero-temperature two-spin Fermi gas. For an initial aspect ratio  $\lambda = 0.05$ ,  $F$  is 0.5. For large anisotropy ( $\lambda \rightarrow 0$ ),  $F$  approaches  $\sim 0.55$ .

So far, we have not considered the effect of the collisions themselves on the momentum distribution. Collisions drive the system towards equilibrium, which corresponds to an isotropic Fermi-Dirac distribution. If this collisional relaxation (Eq. 5) is much faster than the non-equilibrium perturbation due to ballistic expansion (Eq. 2), the momentum distribution maintains local equilibrium at all times. If local equilibrium is maintained, the Boltzmann equation leads to the hydrodynamic equations [30]. For free expansion from anisotropic atom traps, these equations lead to the reversal of anisotropy [16,17]. Even if equilibrium is not fully maintained, collisions always have the effect of transferring momentum from the weakly confining axis to the strongly confining axis resulting in an eventual spatial aspect ratio  $> 1$  [17].

We now want to reconcile our new result that Pauli blocking is inefficient during free expansion, with previous results [26] which show that at low temperatures, collisional damping of collective excitations is suppressed. For this, we derive an equation of motion for the momentum space anisotropy  $\alpha$  to leading order in  $\alpha$  and  $T/T_F$  [31]:

$$\dot{\alpha} = \frac{1}{3}(\partial_x v_x + \partial_y v_y - 2\partial_z v_z) - \frac{n\sigma p_F}{m} C \left( \alpha, \frac{T}{T_F} \right) \quad (6)$$

where  $C$  describes the collisional relaxation and has the asymptotic forms:

$$C\left(\alpha, \frac{T}{T_F}\right) = \frac{3\pi^2}{5} \left(\frac{T}{T_F}\right)^2 \alpha, \quad \alpha \ll \left(\frac{T}{T_F}\right) \\ \frac{96}{49} \alpha^3, \quad \alpha \gg \left(\frac{T}{T_F}\right). \quad (7)$$

In terms of  $\alpha$ , the aspect ratio of the momentum space ellipsoid is  $\sqrt{\frac{1-\alpha}{1+2\alpha}}$ .  $p_F, T, T_F$  are the local Fermi momentum, temperature and Fermi temperature respectively. This equation was derived from the second momentum moment of the Boltzmann equation (Eqs. 4,5), using a Fermi-Dirac distribution with an anisotropic Fermi surface as ansatz [32]. The numerical coefficients in Eq. 7 were obtained by analytic integrations over momentum space.

At zero temperature, there is no linear term in  $\alpha$  in Eq. 7. This shows that Pauli blocking is efficient as long as the anisotropy is small. This is the case for small amplitude excitations in a *trapped* degenerate gas [26]. However, for the large anisotropies of ballistic expansion, the  $\alpha^3$  term, which is independent of temperature and not affected by Pauli blocking, is responsible for collisional relaxation.

Eqs. 6,7 allow us to distinguish collisionless from hydrodynamic behavior in different regimes. The driving term involving  $\mathbf{v}$  is on the order of the trap frequency  $\omega_\perp$  and the damping term has a prefactor  $n\sigma v_F$ . Therefore, the dimensionless parameter characterizing the attainment of the hydrodynamic limit is  $\Phi_0 = n\sigma v_F/\omega_\perp$ . If  $\Phi_0 \ll 1$ , then one can neglect collisions entirely, and the gas will expand ballistically. For small anisotropies, hydrodynamic behavior requires  $\Phi_0(T/T_F)^2 \gg 1$ . For large anisotropies, hydrodynamic behavior requires  $\Phi_0^{1/3} \gg 1$ . At ultralow temperatures, the expansion after release from a highly anisotropic trap may be collisionless initially, but as  $\alpha$  grows, the  $\alpha^3$  term in Eq. 7 will become important, and induce hydrodynamic behavior.

Our calculations clearly predict that for parameters of current experiments,  $\Phi_0 > 1$ , free expansion will not be collisionless, but show behavior which is at least intermediate between collisionless and hydrodynamic [17]. Full hydrodynamic behavior may not be achieved, since for small values of  $\alpha$ , Pauli suppression becomes effective again. More quantitative studies are necessary in order to assess how much this behavior would differ from superfluid expansion. This could be realized by extending analytical studies [17] to high degeneracies or by Monte-Carlo techniques [33]. Our main conclusion is clear, however, that the breakdown of Pauli blocking under free expansion means that hydrodynamic expansion will not be the dramatic, qualitative signal for superfluidity in strongly interacting fermions, the way it was for BEC.

We thank John Thomas, Sandro Stringari, Martin Zwierlein and Aaron Leanhardt for valuable discussions,

and Claudiu Stan and Christian Schunck for critical reading of the manuscript. This work was supported by the NSF, ONR, ARO, and NASA.

- 
- [1] B. DeMarco and D.S. Jin, *Science* **285**, 1703 (1999).
  - [2] A.G. Truscott et. al., *Science* **291**, 2570 (2001).
  - [3] F. Schreck et. al., *Phys. Rev. Lett.* **87**, 080403 (2001).
  - [4] S.R. Granade, M.E. Gehm, K.M. O'Hara, and J.E. Thomas, *Phys. Rev. Lett.* **88**, 120405 (2002).
  - [5] Z. Hadzibabic et. al., *Phys. Rev. Lett.* **88**, 160401 (2002).
  - [6] G. Roati, F. Riboli, G. Modugno, and M. Inguscio, *Phys. Rev. Lett.* **89**, 150403 (2002).
  - [7] K.M. O'Hara et. al., *Science* **298**, 2179 (2002).
  - [8] C.A. Regal and D.S. Jin, *Phys. Rev. Lett.* **90**, 230404 (2003).
  - [9] T. Bourdel et. al., arXiv:cond-mat/0303079 (2003).
  - [10] S. Gupta et. al., *Science* **300**, 1723 (2003).
  - [11] M. Houbiers and H.T.C. Stoof, *Phys. Rev. A* **59**, 1556 (1999).
  - [12] M. Holland, S.J.J.M.F. Kokkelmans, M.L. Chiofalo, and R. Walser, *Phys. Rev. Lett.* **87**, 120406 (2001).
  - [13] M.H. Anderson et. al., *Science* **269**, 198 (1995).
  - [14] K.B. Davis et. al., *Phys. Rev. Lett.* **75**, 3969 (1995).
  - [15] S. Stringari, *Phys. Rev. Lett.* **77**, 2360 (1996).
  - [16] Y. Kagan, E.L. Surkov, and G.V. Shlyapnikov, *Phys. Rev. A* **55**, R18 (1997).
  - [17] P. Pedri, D. Guéry-Odelin, and S. Stringari, arXiv:cond-mat/0305624 (2003).
  - [18] I. Shvarchuck et. al., *Phys. Rev. Lett.* **89**, 270404 (2002).
  - [19] M.A. Baranov and D.S. Petrov, *Phys. Rev. A* **58**, R801 (1998).
  - [20] A. Minguzzi and M.P. Tosi, *Phys. Rev. A* **63**, 023609 (2001).
  - [21] F. Zambelli and S. Stringari, *Phys. Rev. A* **63**, 033602 (2001).
  - [22] C. Menotti, P. Pedri, and S. Stringari, *Phys. Rev. Lett.* **89**, 250402 (2002).
  - [23] G. Ferrari, *Phys. Rev. A* **59**, R4125 (1999).
  - [24] W. Geist et. al., *Phys. Rev. A* **61**, 013406 (1999).
  - [25] M. Holland, B. DeMarco, and D.S. Jin, *Phys. Rev. A* **61**, 053610 (2000).
  - [26] L. Vichi, *J. Low Temp. Phys.* **121**, 177 (2000).
  - [27] W. Geist and T.A.B. Kennedy, *Phys. Rev. A* **65**, 063617 (2002).
  - [28] M.E. Gehm, S.L. Hemmer, K.M. O'Hara, and J.E. Thomas, arXiv:cond-mat/0304633(2003). The authors point out that the suppression of in-trap collisions is not sufficient to guarantee collisionless expansion.
  - [29] G.M. Bruun and C.W. Clark, *Phys. Rev. A* **61**, 061601 (2000).
  - [30] K. Huang, *Statistical Mechanics*, (J. Wiley, New York 1987), 2nd. ed.
  - [31] J.R. Anglin et. al., in preparation (2003).
  - [32] The use of the Fermi-Dirac form neglects possible effects of strong interatomic correlations. Although such effects are not well understood, they are likely to shift a normal degenerate Fermi gas even further away from the colli-

sionless limit.

[33] H. Wu and E. Arimondo, *Europhys. Lett.* **43**, 141 (1998).